

Fibre optic sensing for strain-field measurement in geotechnical laboratory experiments

G. DELLA RAGIONE*, C. N. ABADIE†, X. XU‡§, T. S. DA SILVA BURKE||, T. MÖLLER¶ and E. BILOTTA**

Strain measurement inside the soil body in three-dimensional (3D) experiments is a real challenge for physical modellers in geotechnics. The use of fibre optic sensing offers the possibility of continuous measurement of the strain at depth with high spatial and temporal resolution in small-scale laboratory experiments. Despite the technology not being fully ready yet for centrifuge experiments, this is an important development in geotechnics. This paper explores the capacities of distributed fibre optic sensing (DFOS) as a solution for direct soil strain profile measurement at depth. A series of small-scale plane-strain experiments is used to simulate the simple case of the formation of a downwards subsidence. DFOS cables are laid in the soil specimen, and strains are directly compared with the soil movement, recorded with cameras through particle image velocimetry. Results indicate the ability of DFOS in detecting soil movements and underline the typical signature strain profile expected during this type of experiments. Finite-element analyses are carried out to further underpin the consequences of performing these tests at $1g$ and extend the findings to potential applications in 3D and on the geotechnical centrifuge. This shows promising results for detection of soil strain profiles inside the soil body in 3D.

KEYWORDS: model tests; models (physical); sands; sensors; strain

Emerald Publishing Limited: All rights reserved

INTRODUCTION

Reduced scale physical modelling is an integral part of geotechnical engineering research and enables to further understand aspects of the behaviour of geotechnical systems (Muir Wood, 2004). This typically includes small-scale model tests performed at single gravity on the laboratory floor ($1g$) and at enhanced gravitational field on a geotechnical centrifuge (ng). In both cases, the measurement of physical properties, and in particular stresses and strains, inside the soil body is critical. It enables to elucidate soil–structure interaction, as well as failure mechanisms and infer better design. However, the measurement of the strain field within a particulate media sample has long interested researchers in the field of physical modelling.

To date, elucidating the strain field in geotechnical problems has been successfully achieved by way of particle image velocimetry (PIV), also called digital image correlation (DIC). PIV is an optical technique used to obtain

instantaneous velocity measurement of particles, originally developed for fluid mechanics applications (Adrian, 1991). This technique has been modified and is now routinely used in geotechnical testing to measure the displacement of soil particles between pair of digital images and infer the strain within the soil body in plane-strain conditions (White *et al.*, 2003). The technology and accuracy in the measurements from this technique has evolved massively since the 1990s and has enabled significant progress in physical modelling (Viggiani & Hall, 2012; Take, 2015; Eichhorn *et al.*, 2020). However, this technique requires constructing a model in plane-strain conditions, which uncovers the failure mechanism through a window. It is therefore not suited for performing experiments in three-dimensional (3D), in particular when those experiments contain an asymmetry that render a two-dimensional (2D) plane-strain simplification impossible.

More recently, innovative solutions have emerged to enable the measurement of normal and shear stresses, as well as pore-water pressure inside the soil body. Recent examples used for field testing have been presented by Talesnick (2013) and Templeman (2023). This sort of device would be good candidates for determination of the stress field, which can then be extended to the strain field for small strain experiments. However, these devices are currently too large for accurate measurement of the distributed stress field in small physical modelling experiments.

An alternative solution could however be to use distributed fibre optic cables, laid directly within the soil sample, to acquire the longitudinal strain field along selected critical lines within a soil sample. Fibre optic cables can have very small diameters of the order of 1–2 mm, and therefore do not affect the soil behaviour significantly, nor contribute to reinforcement of the soil sample. Recent developments in fibre optic sensing, and in particular the emergence of the Brillouin optical time-domain reflectometry, enable very high spatial resolution, of a couple to few millimetres, and reasonable sampling frequency to perform very accurate measurements in small-scale physical modelling experiments (Kechavarzi *et al.*, 2016).

Manuscript received 6 June 2023; accepted 12 October 2023.
First published online at www.geotechniqueletters.com on 23 October 2023.

*Department of Civil Engineering, University of Naples, Naples, Italy; formerly CSIC, Cambridge, UK.

†Département Géotechnique, Environnement, Risques Naturels et Sciences de la Terre, Université Gustave Eiffel, France christelle.abadie@univ-eiffel.fr (Orcid:0000-0002-5586-6560).

‡Department of Engineering, University of Cambridge, Cambridge, UK.

§Cambridge Centre for Smart Infrastructure and Construction (CSIC), Cambridge, UK.

||Department of Civil Engineering, University of Pretoria, Pretoria, South Africa (Orcid:0000-0001-9393-8601).

¶Department of Engineering, University of Cambridge, Cambridge, UK.

**Department of Civil Engineering, University of Naples, Naples, Italy; formerly CSIC, Cambridge, UK (Orcid:0000-0002-3185-2738).

This paper aims at exploring the use of distributed fibre optic sensing (DFOS) for measurement of the strain field in physical modelling experiments in geotechnics. The paper provides a simple pilot study that demonstrates the performance of using direct fibre optic sensing cables within the soil media to obtain a profile of the strain field in 3D. The paper also highlights the limitations of using this technology at low stress levels for $1g$ experiments, compared with representative centrifuge experiments, which benefit from the enhanced gravitational field. This study was conducted as part of the SINKhole Early Warning (SINEW) project, which aims at identifying an early warning system for sinkhole expansion.

METHODOLOGY

This paper explores the potential use of fibre optic sensing in physical modelling experiments by performing a very simple test at $1g$ in plane-strain conditions, and comparing the strain measured by the fibre optic cable with the results from PIV. The extension to 3D experiments is modelled through finite-element analyses, which offers more flexibility for detailed analysis inside the soil body.

The most promising type of fibre optic sensing for geotechnical physical modelling, employs Brillouin optical time-domain reflectometry (BOTDR). A laser pulse is emitted by an interrogator through the fibre and the location and amount of axial deformation within the cable is inferred by measuring the proportional relationship between the Brillouin frequency shift of the backscatter light. This permits very high spatial resolution over small distances, suitable for laboratory applications. Unfortunately, at the time where this study was undertaken, the use of such analysers on the geotechnical centrifuge was not yet mature

(Eichhorn, 2021). Performing tests at $1g$, coupled with predicted scaling for applications on the geotechnical centrifuge using 3D finite-element analyses, was therefore selected as a good compromise to explore the potential of using this technology for direct soil strain measurement for future applications in physical modelling experiments.

Experimental set-up

The experimental study presented in this paper was performed at $1g$ using a 790×200 mm rectangular rig, equipped with a plane strain trapdoor of width, $B = 100$ mm that can mimic the formation of a sinkhole, as shown in Fig. 1(a). The tests were conducted using Hostun sand, with an average particle size, $d_{50} = 0.356$ mm. A sample of height $H = 200$ mm was prepared, with relative density $D_R = 52\%$. The sand was poured using an automatic sand pourer, and careful consideration of scaling shows that the medium dense sample prepared at $1g$ in this paper is most representative of the behaviour of a much denser sand profile. In the type of experiments conducted in this paper, most of the failure mechanism is driven by the strength and dilatancy of the sand, which means that appropriate scaling of the dilatancy angle is needed (Möller *et al.*, 2023). The dependency of the dilatancy of sand on the mean effective stress p' and the relative density D_R of the soil, is best accounted for through the relative dilatancy index I_R (Bolton, 1986):

$$I_R = D_R(Q - \ln p') - R \quad (1)$$

where Q and R are two fitting parameters which are a function of the soil material (Chakraborty and Salgado, 2010), commonly set equal to 10 and 1, respectively. Using

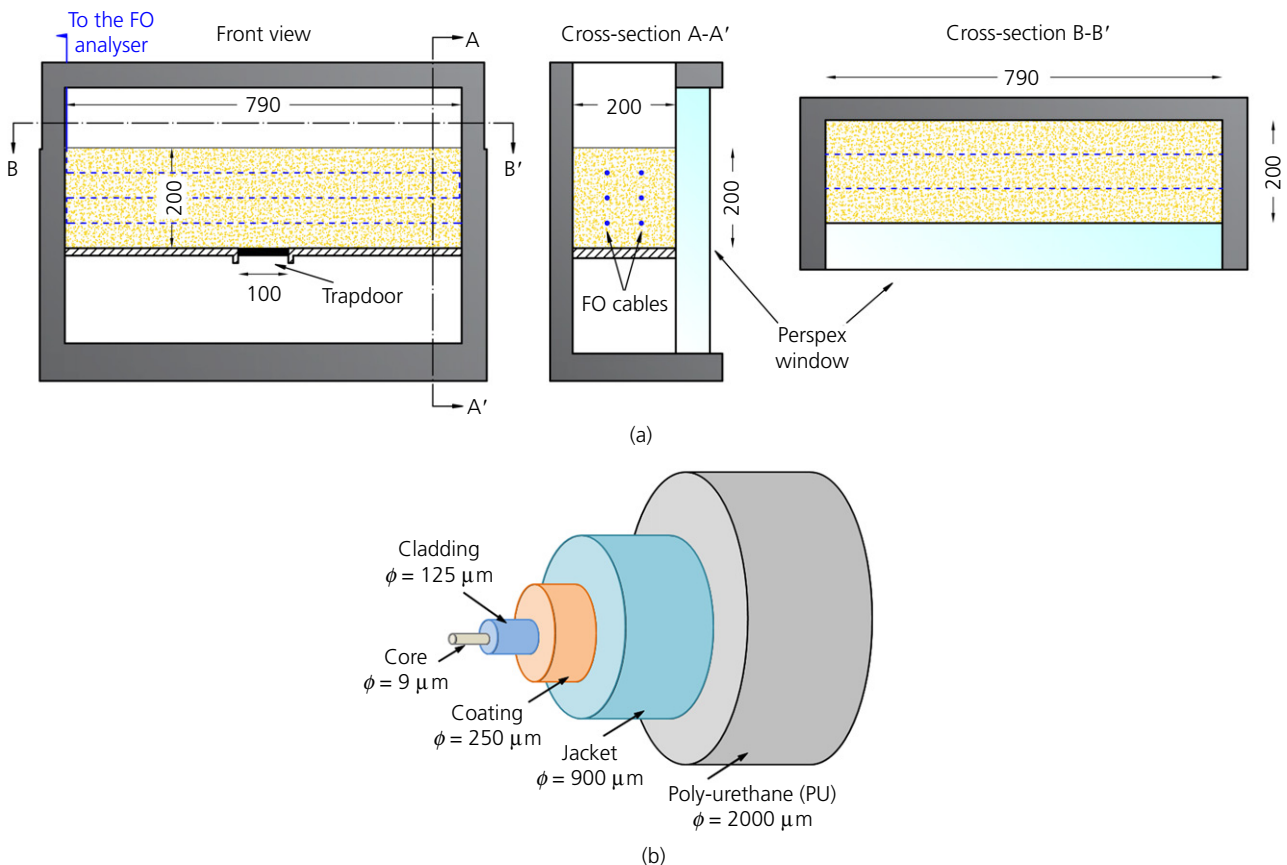


Fig. 1. (a) Experimental rig with plane strain trapdoor (dimensions in mm), (b) schematic representation of experimental strain sensing cable cross-section

this relationship, the $1g$ tests shown in this paper at $D_R = 52\%$ best capture the dilatancy behaviour of a real soil at approximately $D_R = 80\%$ at the trapdoor level, with $I_R = 3.6$ (Möller *et al.*, 2023).

Fibre optic cables were laid away from the window and within the soil body, at three different heights $z = 50, 100$ and 150 mm above the trapdoor level. These specific layers were highlighted using dyed black sand on the window front to facilitate the visibility of the shear band during failure (Fig. 2(a)).

A 2 mm in diameter tight-buffed polyurethane-coated fibre optic strain sensing cable manufactured by Suzhou Nanzee Sensing Co., Ltd, was used in this study, with a single fibre optic core (Fig. 1(b)). This fibre is a common single-mode fibre (SMF) that has been widely used in fibre-optic communication and structural health monitoring applications. It is however, only able to measure axial strain. Due to its relatively low modulus, it can be easily pre-strained and directly integrated into loose material such as soil. It is well suited for the experiments proposed in this paper, with a yield stress of 23.1 MPa and yield strain of 6.7%. Extensive laboratory calibration tests performed at the Cambridge Centre for Smart Infrastructure and Construction (CSIC) has demonstrated its perfect strain transfer behaviour (e.g. strain transfer coefficient 20 080 $\mu\epsilon/\text{GHz}$ by way of BOTDR analyser and 6.67 $\mu\epsilon/\text{GHz}$ by way of Luna OFDR ODiSI 6100 analyser). Previous physical model tests and field monitoring projects have also confirmed its satisfactory strain transfer performance for field applications. The cables were pinned at the edge of the box, with no additional slack to permit strain relief beyond interface friction failure and the 2 mm cables were coated in sand to maximise soil–cable interface coupling (Xu *et al.*, 2022). The cables were laid 60–70 mm

away from the window, and therefore, are here unlikely to impact the soil deformation measurably.

The DFOS Luna ODiSI 6100 analyser was used to collect wavelength changes, converted into differential strain changes within the cable, with the method described by Kechavarzi *et al.* (2016). This analyser is very well adapted for small-scale experiments in the laboratory due to the small spatial resolution and precise gauge length (2.6 mm used in this case). Strain obtained from the DFOS cables were compared to soil strain profiles measured through particle imaging through the window, and acquired using a pair of Canon Powershot G10 cameras and analysed with GeopIV_RG (Stanier *et al.*, 2015). With a sample width of $L = 790$ mm, this provides ~ 300 sampling points in the fibre optic cable at each level, enabling the establishment of a precise continuous distributed strain profile.

Finite-element analysis

Finite-element analyses were carried out using Plaxis3D to further analyse the experimental results obtained at $1g$ and extend the findings to realistic stress levels in both 2D and 3D that could be obtained in the future on the geotechnical centrifuge. The domain consisted in half of the soil specimen in order to reduce computational effort. The material model used for the soil was the hardening soil model with small strain stiffness (HSsmall; Schanz and Vermeer, 1996; Benz, 2009). The incorporation of this material model is particularly suitable for trapdoor tests characterised by small deformations, since it captures the reduction of soil stiffness with increasing strain during the early stages of the trapdoor test. The cables were modelled as embedded beams with an interface associated and the material model used was a perfect elastic behaviour, with a Young's modulus of

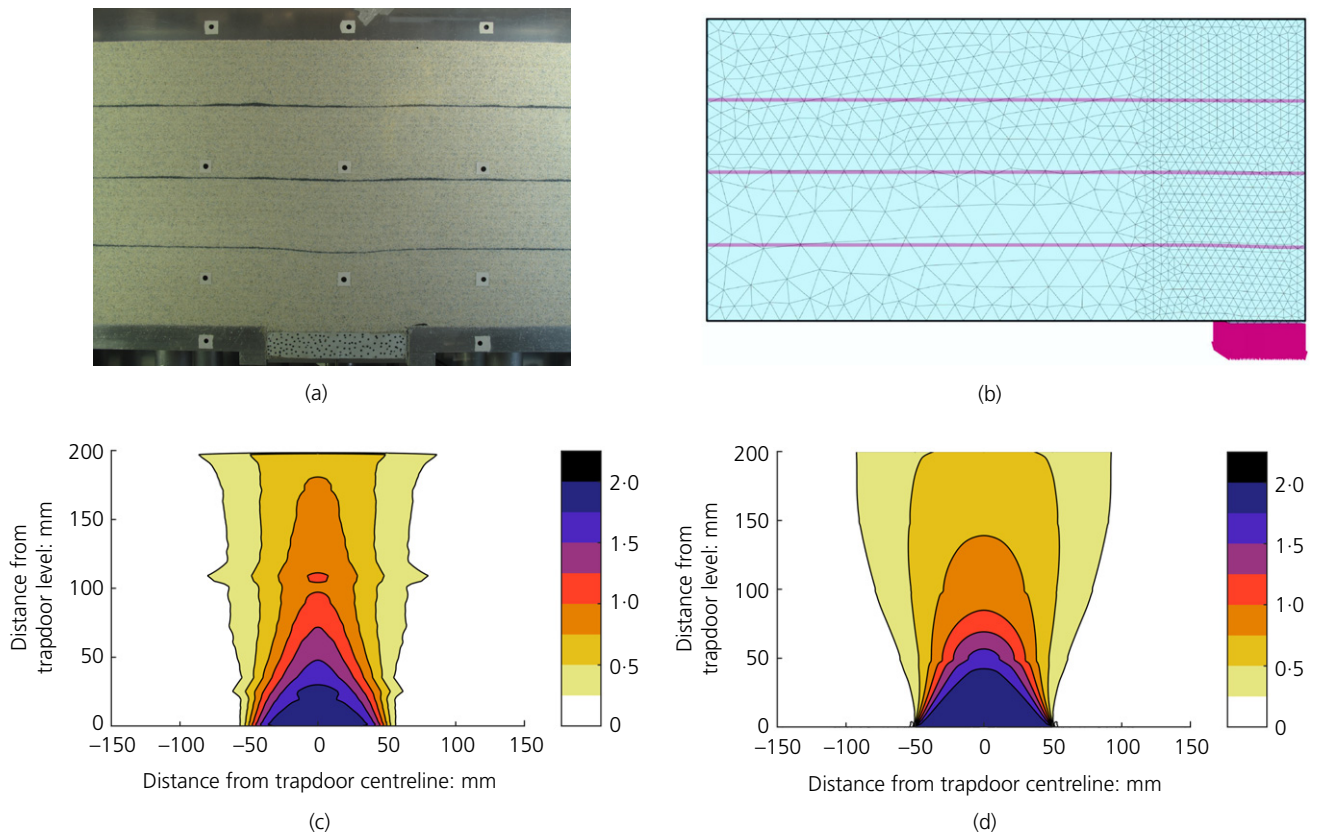


Fig. 2. (a) Image acquired from the Canon Powershot G10, used for PIV analysis; (b) experimental contour plot of vertical displacements from PIV; (c) numerical half-space deformed mesh; (d) numerical contour plot of vertical displacements ($D_R = 52\%$ $\delta = 2$ mm)

200 MPa. Full and loose coupling between the cable and the soil were both assumed to model the best- and worst-case scenario that could be obtained in practice. Further detail on the numerical models is described in Della Ragione *et al.* (2023).

RESULTS

For a trapdoor displacement δ lower or equal to 1–2% of the trapdoor width, the soil is able to adjust and redistribute the stresses on an adjacent support (da Silva Burke & Elshafie, 2021). This behaviour is known as arching and is regarded as the early phase of the subsidence formation. This phase was selected to validate the feasibility of using DFOS to measure soil strain in the soil body due to the small strain generated,

which are therefore more challenging to measure. Despite logging the strain profile at three heights within the soil sample, most of the results shown in the following apply to the cable closest to the surface, which, due to an increased lack of coupling between the soil and the cable, is also the most challenging to measure.

Validation of scientific method

The main results from PIV analyses consist in the displacement fields above the trapdoor. Contour plots of displacements, together with the deformed shape of the soil sample and cables, are compared for validation of the numerical model in Fig. 2. The observed trends show good agreement in the development of the mechanism.

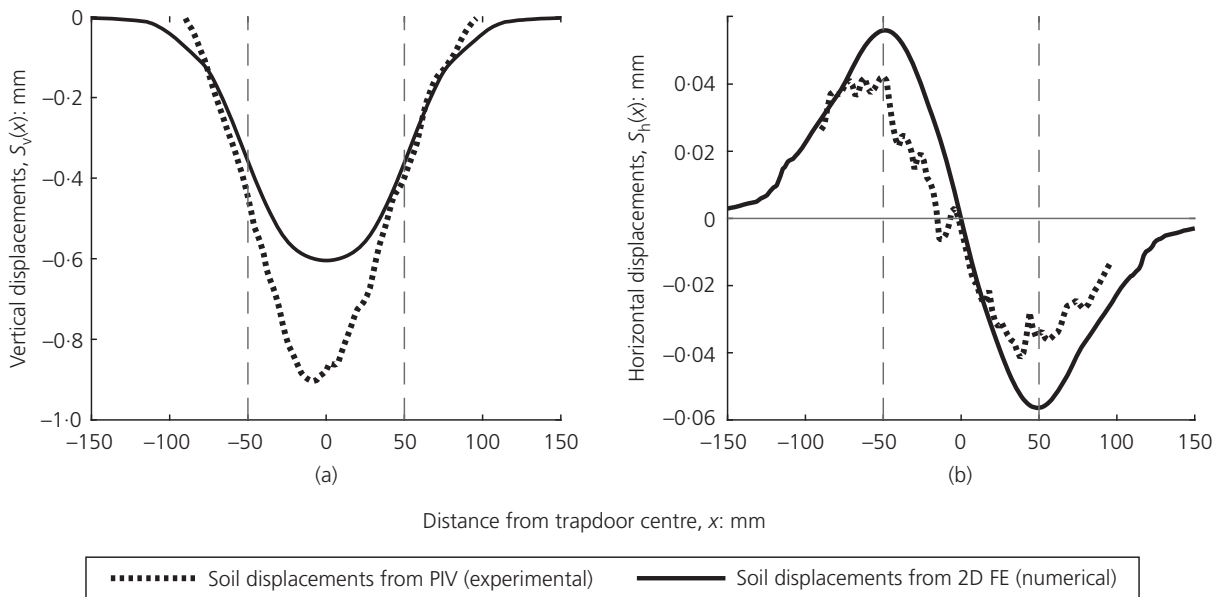


Fig. 3. (a) Vertical displacements from PIV and numerical results, (b) horizontal displacements from PIV and numerical results ($D_R = 52\%$ $\delta = 2$ mm and $z = 150$ mm)

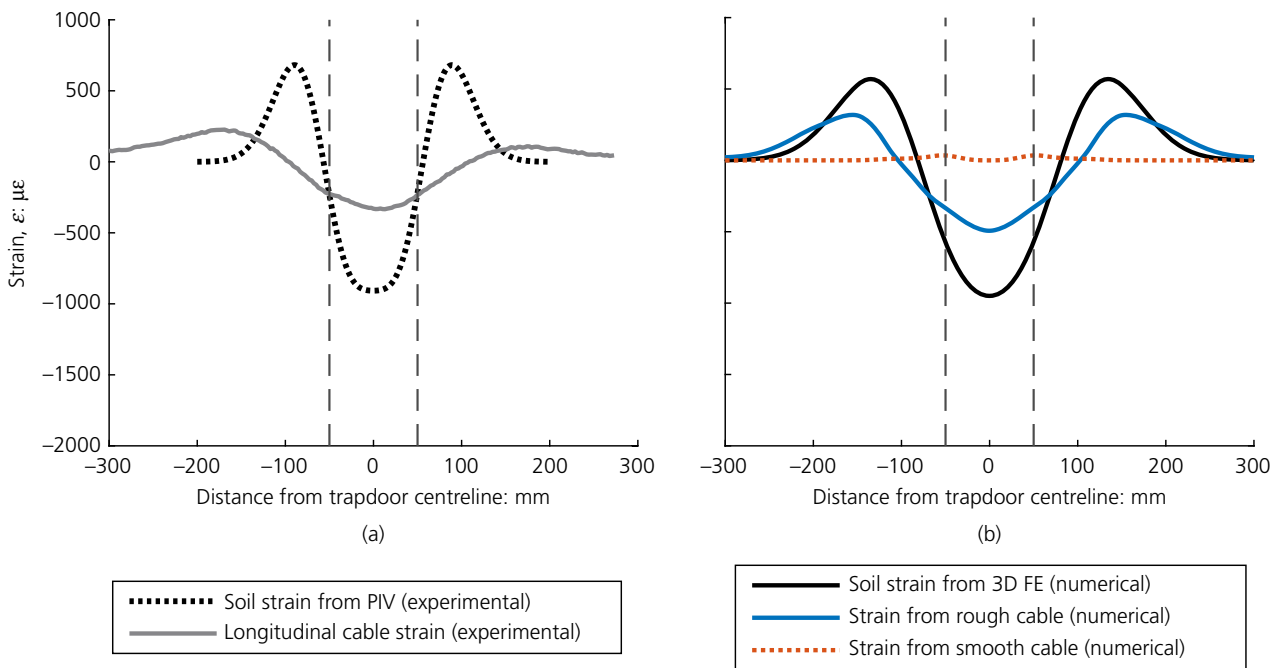


Fig. 4. (a) Soil strain from PIV and strain within the fibre optic cable; (b) numerical horizontal soil strain, rough and smooth cables numerical strain (1g test, $D_R = 52\%$, $\delta = 2$ mm and $z = 150$ mm)

To further this observation, individual layers are analysed more closely. The settlement profiles $S_v(x)$ is fitted using a modified Gaussian distribution following recommendations by da Silva (2018) and Möller *et al.* (2023). Horizontal soil displacements $S_h(x)$ from PIV are interpolated using a double Gaussian distribution to obtain the displacement profiles from PIV shown in Fig. 3. Detail on the processing method is provided in depth in Möller *et al.* (2023). The experimental data are compared with the numerical results, showing good agreement with the experimental data and validating the numerical model. It is important to note the difference in magnitude between horizontal and vertical displacements obtained in both the experimental and numerical cases.

Performance of fibre optic cables at 1g

From the soil displacement profiles, it is then possible to evaluate the strain, which are representative of those experienced by the fibre optic cable using:

$$\varepsilon(x) = \frac{\sqrt{(x_{i+1} - x_i + S_{h,i+1} - S_{h,i})^2 + (S_{v,i+1} - S_{v,i})^2}}{x_{i+1} - x_i} - 1 \tag{2}$$

where x is the abscissa at which the displacements are considered, S_h and S_v are the horizontal and vertical displacements. The experimental soil strain evaluated from the fitted displacement profiles are compared with the experimental strain experienced by the fibre optic cables, and obtained from the Luna ODiSI 6100 interrogator.

Figure 4(a) therefore shows compared strain profile between the PIV measurement and the DFOS signal. The graph shows a fairly good agreement in the trends acquired from the DFOS, which exhibit a very distinct signature strain profile that corresponds to the strain profile observed for the expansion of a subsidence.

Figure 4(a) also highlights a difference in strain magnitude between the fibre optic cable and the corresponding strain in the soil, coupled with a difference in trough width of this

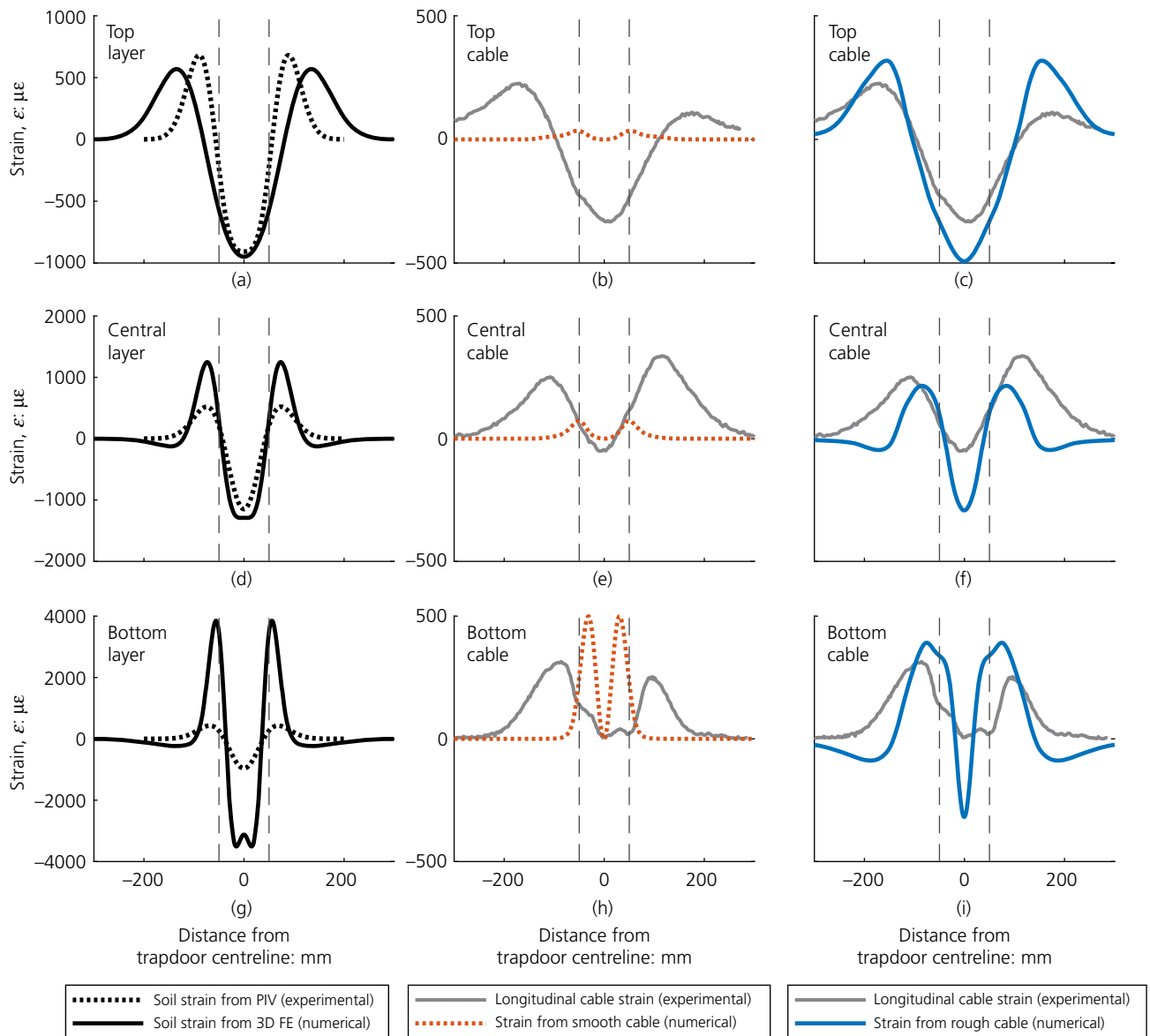


Fig. 5. (a), (d), (f), Experimental (PIV) against numerical soil strain profiles for top, central and bottom layers, respectively; (b), (e), (h) experimental (DFOS) against numerical smooth cable strain profiles for top, central and bottom cables, respectively; (c), (f), (i) experimental (DFOS) against numerical rough cable strain profiles for top, central and bottom cables, respectively (1g test, $D_R = 52\%$, $\delta = 2$ mm)

same profile. This difference is due to a lack of shear transfer between the soil and the cable, induced by a lack of coupling. The results shown here are for the top cable, which is the most severely impacted by the lack of confining pressure at $1g$. The results shown in this figure therefore prove that DFOS is still able to provide reasonable understanding of the soil strain profile.

The difference in trough width can also be further explained by friction between the sand particles and the window, which very often alter the PIV results from the true soil strain. This is indeed what likely perturbs the results from Fig. 2(b) at each layer where sand was inked in black. To further understand what the true soil and cable strain are and whether the readings from DFOS can be improved for $1g$ experiments, further inspection of the fibre optic cable is performed using the numerical model. Figure 4(b) shows the compared soil strain profile with the best- and worst-case scenarios where perfect and null coupling between the soil and cable would be achieved, respectively. This is extended to all soil layers in Fig. 5, where the middle and bottom cables benefit from slightly more confining pressure at $1g$. It clearly shows that the

results at $1g$ obtained during the experimental campaign are already very good and cannot be improved massively.

Curiously, the results in Fig. 5(h) show larger strain for the smooth cable than for the rough cable. This is explained by looking at the horizontal and vertical components of the strain from equation (2) recalling that horizontal displacement induced by trapdoor opening induces compressive horizontal strain in the soil just above it. For a smooth cable, no horizontal displacements are induced in the cable by soil movements, and only vertical displacements are hence generated, inducing pure tensile strain (i.e. positive strain) in equation (2). In contrast, for the rough cable, soil movements induce both vertical and horizontal displacements in the cable, which induce both positive and negative strains and reduce the maximum amount of tensile strain found for the smooth cable.

Potential use fibre optic sensing for 3D centrifuge experiments

Finally, the numerical model is used to extend the results to a potential centrifuge experiment, performed at $40g$ in 3D,

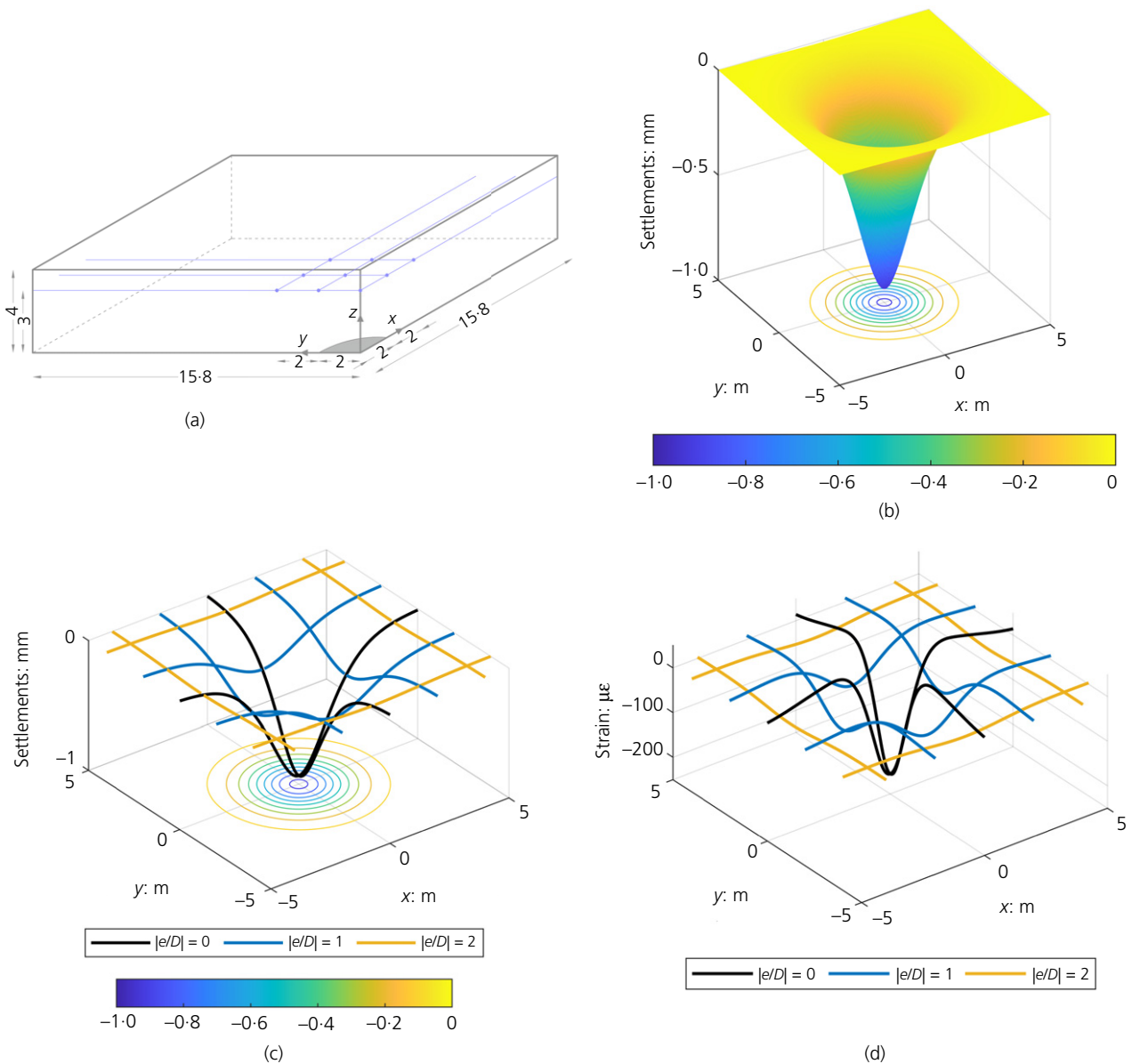


Fig. 6. (a) Schematic representation of 3D model in axial symmetric condition (dimensions in m); (b) soil settlements at $z = 3$ m above circular trapdoor; (c) rough cables settlements at $z = 3$ m above circular trapdoor; (d) rough cables strain profile at $z = 3$ m above circular trapdoor ($\delta = 40$ mm)

and with a relative density $D_R = 87.5\%$. The test very much corresponds to one of the centrifuge tests performed by da Silva (2018), but is here extended to a 3D circular trapdoor, schematised in axisymmetric conditions in Fig. 6(a).

Figure 6(b) shows the settlement profile obtained for a layer located 3 m below the soil surface. This is compared with the settlement profile derived from the grid of fibre optic cables, shown in Fig. 6(c) of the cable. The figure shows very good agreement between both profiles, and demonstrates that the loss of magnitude and distortion of the profile, observed at $1g$, resorbs at higher g -levels. To conclude, Fig. 6(d) shows the strain grid that would have been obtained in a 3D physical modelling experiment at a specific height, and from which the strain field can be obtained by way of interpolation, providing further insight into the soil behaviour.

CONCLUSIONS

The use of DFOS can improve experimental testing in geotechnics by enabling the measurement of small strain with a high level of spatial and temporal accuracies in a relatively limited spaced sample at depth. Different from civil structural applications (e.g. concrete structures, steel structures etc.), where the fibre can be simply glued onto the surface, the effectiveness of DFOS in following soil movements is strongly dependent from the soil–cable interface and this limit has been considered as the main barrier to the use of this technology for geotechnical applications. This is particularly true for tests at $1g$ on the laboratory floor where the stress level is low, and impact coupling great.

This paper illustrates the effectiveness of a relatively new technology (i.e. DFOS with Raileigh backscattering), and not yet available for tests on the geotechnical centrifuge, for sensing soil movement in $1g$ small-scale experiments. The study is focused on a simple plane-strain small-scale trapdoor test, performed in controlled conditions at $1g$, where soil strain measured from PIV can be directly compared with DFOS data. The results demonstrate a clear ability of the DFOS in measuring accurately the correct strain profile trend, for very small movements induced in the soil. In this experiment, DFOS is able to pick up an unequivocal profile of strain, induced by the trapdoor movement, right from the beginning of the test – that is, for trapdoor movement $\delta \leq 0.01\text{--}0.02$ B. This is a very promising result for geotechnical testing at $1g$. However, an order of magnitude difference between the DFOS and the PIV is also observed.

The key limitations of the use of fibre optic at $1g$ is the very large contrast of stiffness between the cable (axial stiffness) and the soil, which results in a non-conformity in the cable deformation compared to the soil movement. For this reason, the cable strives to conform to the soil movement in horizontal (longitudinal) direction, regardless of its surface roughness, as demonstrated by the numerical analyses. This in turn provides a loss of precision on the width of the failure mechanism, and its magnitude, while preserving its overall shape. At larger depth with larger confining stresses, as well as for experiments on the geotechnical centrifuge, the soil stiffness is larger and the contrast of stiffness with the cable reduces. The cable therefore conforms much better the actual soil strain. Further research could explore how to improve this result using a multi-core fibre optic cable (MCF) that would enable the measurement of bending strain.

This does not invalidate the use of DFOS for $1g$ small-scale experiments, and DFOS can be used to provide locations in extremum of the strain and reveal the position of a subsidence. Nevertheless, tests at higher confining stresses, it seems that real scale (on site) measurements or those in centrifuge are much more suitable for the use of DFOS.

For this reason, numerical analyses are used to extend the findings to potential future applications for 3D experiments on the geotechnical centrifuge. The numerical results prove that DFOS technology is a promising technology to further understand soil strain and movement at depth in geotechnical experiments. This paper also shows that, in the near future, predicting the response of the fibre optic by way of finite-element analyses prior to performing tests in the laboratory is probably a very good route to better understand the fibre optic strain measurements recorded during the test.

ACKNOWLEDGEMENTS

The authors are grateful to CSIC (EPSRC (EP/N021614/1) and Innovate UK (920035)) for funding and supporting this work and Dr Jennifer Schooling and Professor Giulia Viggiani for facilitating the collaboration between the University of Naples Federico II and the University of Cambridge. They are also thankful to the Schofield Centre and its director, Professor Gopal Madabhushi, for their support with the laboratory experiments. Fruitful advice and discussion with Professor Malcolm Bolton, Professor Sadik Oztoprak, Professor Giulia Viggiani were also very valuable for the development of this project.

REFERENCES

- Adrian, R. J. (1991). Particle imaging techniques for experimental fluid mechanics. *Ann. Rev. Fluid Mech.* **23**, 261–304, <https://doi.org/10.1146/annurev.fl.23.010191.001401>.
- Benz, T. (2006). *Small-strain stiffness of soils and its numerical consequences*. PhD thesis, University of Stuttgart, Stuttgart, Germany.
- Bolton, M. D. (1986). The strength and dilatancy of sands. *Géotechnique* **36**, No. 1, 65–78, <https://doi.org/10.1680/geot.1986.36.1.65>.
- Chakraborty, T. & Salgado, R. (2010). Dilatancy and shear strength of sand at low confining pressures. *J. Geotech. Geoenviron. Eng.* **136**, No. 3, [https://doi.org/10.1061/\(ASCE\)GT.1943-5606.0000237](https://doi.org/10.1061/(ASCE)GT.1943-5606.0000237).
- da Silva Burke, T. S. & Elshafie, M. Z. E. B. (2021). Arching in granular soils: experimental observations of deformation mechanisms. *Géotechnique* **71**, No. 10, 866–878, <https://doi.org/10.1680/jgeot.19.P174>.
- da Silva, T. S. (2018). *Centrifuge modelling of behaviour of geosynthetic-reinforced soils above voids*. PhD thesis, University of Cambridge, Cambridge, UK.
- Della Ragione, G., Bilotta, E., Xu, X., da Silva Burke, T. S., Möller, T. & Abadie, C. N. (2023). Numerical investigation of fibre optic sensing for sinkhole detection. *Géotechnique* **1–14**, <https://doi.org/10.1680/jgeot.22.00241>.
- Eichhorn, G. N. (2021). *Landslide–pipeline interaction in unsaturated silty slopes*. PhD thesis, University of Cambridge, Cambridge, UK.
- Eichhorn, G. N., Bowman, A., Haigh, S. K. & Stanier, S. (2020). Low-cost digital image correlation and strain measurement for geotechnical applications. *Strain* **56**, e12348, <https://doi.org/10.1111/str.12348>.
- Kechavarzi, C., Soga, K., De Battista, N., Pelecanos, L., Elshafie, M. Z. E. B. & Mair, R. J. (2016). *Distributed fibre optic strain sensing for monitoring civil infrastructure*. ICE Publishing, London, UK.
- Möller, T., da Silva Burke, T. S., Xu, X., Della Ragione, G., Bilotta, E. & Abadie, C. N. (2023). Distributed fibre optic sensing for sinkhole early warning: experimental study. *Géotechnique* **73**, No. 8, 701–715, <https://doi.org/10.1680/jgeot.21.00154>.
- Muir Wood, D. (2004). *Geotechnical modelling*, 1st edn. Boca Raton, FL, USA: CRC Press.
- Schanz, T. & Vermeer, P. A. (1996). Angles of friction and dilatancy of sand. *Géotechnique* **46**, No. 1, 145–151, <https://doi.org/10.1680/geot.1996.46.1.145>.
- Stanier, S. A., Blaber, J., Take, W. A. & White, D. J. (2015). Improved image-based deformation measurement for geotechnical

- applications. *Can. Geotech. J.* **53**, 727–739, <https://doi.org/10.1139/cgj-2015-0253>.
- Take, A. W. (2015). Thirty-sixth Canadian geotechnical colloquium: advances in visualization of geotechnical processes through digital image correlation. *Can. Geotech. J.* **52**, No. 9, 1199–1220, <https://doi.org/10.1139/cgj-2014-0080>.
- Talesnick, M. (2013). Measuring soil pressure within a soil mass. *Can. Geotech. J.* **50**, No. 7, 716–722, <https://doi.org/10.1139/cgj-2012-0347>.
- Templeman, J. O. (2023). *Measurement and modelling of soil-structure interaction for open caisson shafts*. DPhil thesis, Department of Engineering Science, University of Oxford, Oxford, UK.
- Viggiani, G. & Hall, S. A. (2012). Full-field measurements in experimental geomechanics: historical perspective, current trends and recent results. In *ALERT Doctoral school 2012: advanced experimental techniques in geomechanics* (eds C. Viggiani, S. Hall and E. Romero), pp. 3–67.
- White, D. J., Take, W. A. & Bolton, M. D. (2003). Soil deformation measurement using particle image velocimetry (PIV) and photogrammetry. *Géotechnique* **53**, No. 7, 619–631, <https://doi.org/10.1680/geot.2003.53.7.619>.
- Xu, X., Abadie, C. N., Möller, T., Della Razione, G. & da Silva Burke, T. S. (2022). On the use of high-resolution distributed fibre optic sensing for small-scale geotechnical experiments at 1g. *Proceedings of the 10th International conference on physical modelling in geotechnics (ICPMG)*, Daejeon, South Korea, <https://doi.org/10.17863/CAM.92635>.

HOW CAN YOU CONTRIBUTE?

To discuss this paper, please submit up to 500 words to the editor at support@emerald.com. Your contribution will be forwarded to the author(s) for a reply and, if considered appropriate by the editorial board, it will be published as a discussion in a future issue of the journal.